Electronic Supplementary Material (ESI) for ChemComm.

Supporting Information

Facile One-pot Synthesis of MoS_2 Quantum Dots/Graphene/TiO_2 Composites for Highly Enhanced Photocatalytic Property

Weiyin Gao,[†] Minqiang Wang,,[†] Chenxin Ran,[†] Le Li[†]*

[†]Electronic Materials Research Laboratory, Key Laboratory of Ministry of Education, School of Electronic and Information Engineering, International Centers for Dielectric Research, Xi'an Jiaotong University, Xi'an 710049, China

Experimental detail

Chemicals. GO was prepared from natural graphite (Wodetai Ltd. Co., Beijing, China, 99.9%) by a classical Hummers method with some modification.[1, 2] $Na_2MoO_4 \cdot 2H_2O$ and thiocarbamide (A.R. ≥99.8%) was purchased from Xi'an chemical reagent factory. TiO_2 (P25, 20% rutile and 80% anatase) was purchased from Degussa. Other solvents were used directly as received without further purification. The experiments were carried out at room temperature and humidity.

Synthesis of GO. First, GO was synthesized by the modified Hummers' method. In a typical synthesis, 3 g graphite powder was put into an 80 °C solution of 12 mL concentrated H_2SO_4, 2.5 g $K_2S_2O_8$, and 2.5 g P_2O_5. Then the mixture was kept at 80 °C for 5 h in a water bath. Successively, the mixture was cooled to room temperature and diluted with 500 mL H_2O and left overnight. After that, the mixture was filtered and washed with H_2O using a 0.45 μm Millipore filter to remove the residual acid. Then the product was dried in a vacuum oven at room temperature. This pre-oxidized graphite was then subjected to oxidation by Hummers' method described as follows. Pre-oxidized graphite powder was put into cold (0 °C) 120 mL concentrated H_2SO_4. Then, 15 g $KMnO_4$ was added 1 g at a time under stirring and the temperature of the mixture was kept to be below 20 °C by cooling in ice. Successively, the mixture was stirred at 35 °C for 2 h, and then carefully diluted with 250 mL of H_2O. After that, the mixture was stirred for another 2 h, and then additional 700 mL of H_2O was added under stirring followed by 20 mL of 30% H_2O_2. The resulting brilliant-yellow mixture was filtered and washed with 10 wt% HCl aqueous solution (1000 mL) to remove metal ions and washed repeatedly with H_2O to remove the acid until the pH of the filtrate was neutral. The resulting GO slurry was dried in a vacuum oven at 60 °C.

Synthesis of MoS_2 (QDs)/Graphene/TiO_2. MoS_2 (QDs)/Graphene/TiO_2 was prepared by an efficient one-pot solvothermal method under atmospheric pressure. In a typical synthesis, 20 mL DMAc was added into 20 mL GO aqueous dispersion (0.5 mg/mL), where the volume ratio between DMAc and H_2O was

1:1, and mixed under magnetic stirring. Meanwhile, 0.151 g of $Na_2MoO_4 \cdot 2H_2O$ and 0.0475 g thiocarbamide were dissolved in 5 mL of distilled water, and stirred for 10 min to ensure complete mixing, then the mixed homogeneous aqueous solution was put in the prepared GO solution drop by drop. Next, 2 g P25 powder were added into the above solution and stirred for 10 min to ensure complete mixing. And then, the reaction was allowed to proceed under magnetic stirring at 150 °C in oil bath for 10 h. Finally, the product was washed with distilled water and ethyl alcohol twice and filtered through a 0.45 μm Millipore filter, the resulting precipitate was then re-dispersed into ethyl alcohol and stored at room temperature for characterization. In our previous work, we discussed the effect of the graphene content in the graphene/TiO_2 hybrid photocatalyst on the photocatalytic activity, and we found that the optimum weight ratio between graphene and TiO_2 was 1:200. So in this work the weight ratio between TiO_2 and graphene is kept the same that is, 200:1.[3] A series of MoS_2/r-GO/TiO_2 composites were synthesized by varying the content of precursor of MoS_2 to investigate the optimum ratio of MoS_2. The detailed reaction conditions were listed in Table S1.

Materials Characterization

Diffuse reflectance absorption spectra and ultraviolet-visible (UV−vis) spectra were recorded on a Jasco V-570 UV/vis/NIR spectrophotometer at room temperature. **X-ray photoelectron spectroscopy (XPS)** (Escalab 250Xi, Thermo Fisher Co., USA) measurement was processed using an Al-Ka monochromatic X-ray source (1486.6 eV). **Nitrogen adsorption-desorption isotherm measurements** were conducted at 77 K (SSA-4330, Builder Ltd. Co., Beijing, China). **X-ray diffraction (XRD) analyses** were performed on a XRD-6000 (Japan) with Cu Kα (1.5406 Å) radiation. The diffraction data was recorded for 2Θ angles between 5° and 80°. **Transmission electron microscopy (TEM) and high-resolution TEM (HRTEM) images** were obtained with a JEM-2100 transmission electron microscope (Japan Electron Optics Labortary Co., Ltd., JEOL) with an accelerating voltage of 200 kV. The sample for TEM characterization was prepared by placing a drop of prepared solution on carbon-coated copper grid and drying at room temperature. **Raman spectra** were investigated using a JY LabRAM HR800

laser Raman spectrometer from 100 to 3000 cm^{-1} at room temperature.

Photodegradation experiment. The photocatalytic degradation pollutant experiment was performed by measuring the photodegradation of Rh B solution under simulated solar irradiation at ambient temperature. Briefly, 40 mg of catalyst was dispersed in 80 mL of 10 mg/L Rh B solution under ultrasonication for 10 min. Before illumination, the mixture was magnetically stirred for 60 min in the dark to establish an adsorption–desorption equilibrium of the pollutant with the catalyst. A solar simulator with 150 W Xe lamp (Sciencetech Inc., SS-150) was used as the light source. The experimental solution was placed in a quartz bottle, 10 cm from the light source. At given intervals, 5 mL of the suspension was withdrawn and centrifuged to remove the dispersed catalyst powder. The concentration of the clean transparent solution was determined by measuring the 554 nm absorbance of Rh B using a spectrophotometer (Jasco V-570, Shimadzu, Japan). For the stability test of MGT in photodegradation of Rh B under simulated solar light, six consecutive cycles were tested. At the beginning, 40 mg of MGT was dispersed in 80 mL of Rh B solution (10 mg/L). Then the mixture underwent six consecutive cycles, each lasting for 100 min.

Trapping tests for radicals and holes. The trapping experiments for photogenerated radicals and holes were carried out using tertbutanol (t-BuOH, radical scavenger) and ethylenediaminetetraacetic acid disodium salt (EDTA-2Na; hole scavenger). For the trapping of photogenerated radicals, 0.059 g t-BuOH was dispersed in 80 mL of 10 mg/L Rh B solution under ultrasonication for 10 min. And then 40 mg of catalyst was dispersed into the prepared solution under ultrasonication for 10 min. The next step in the experimental process was the same as that in the above photocatalytic tests. For the hole trapping experiments, the experimental procedure was similar to the radical one, except that 0.268 g EDTA-2Na was used instead of t-BuOH.

Fig.s

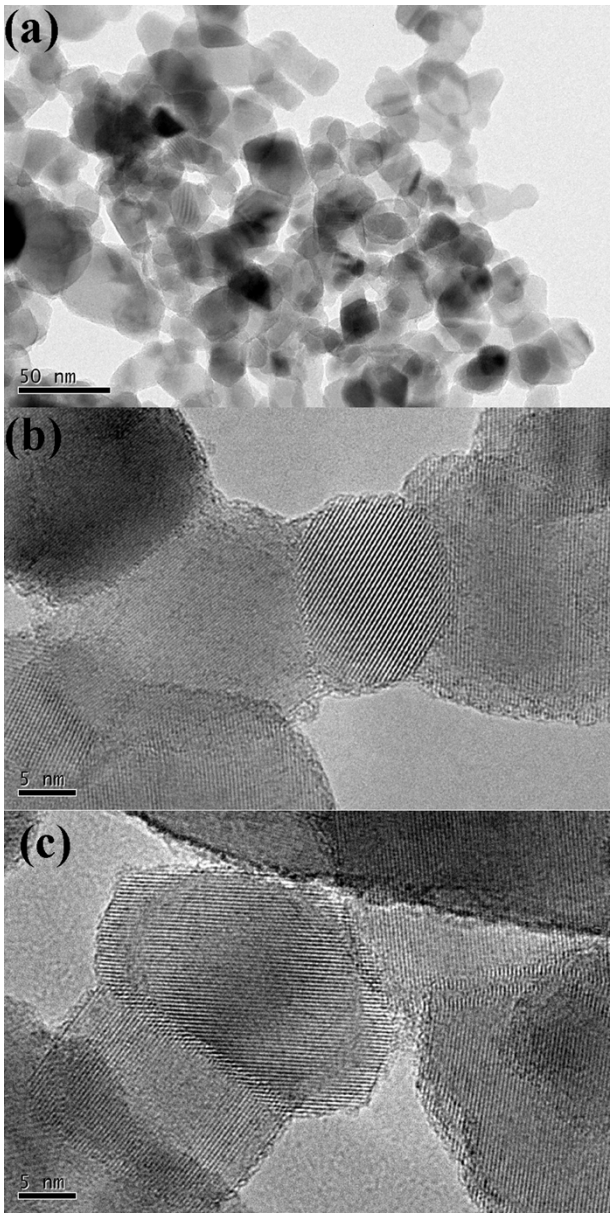

Fig. S1 (a) TEM and (b), (c) HRTEM image of MoS_2/TiO_2 composite, it shows no MoS_2 QDs, which indicates the important role of GO in the formation of MoS_2 QDs.

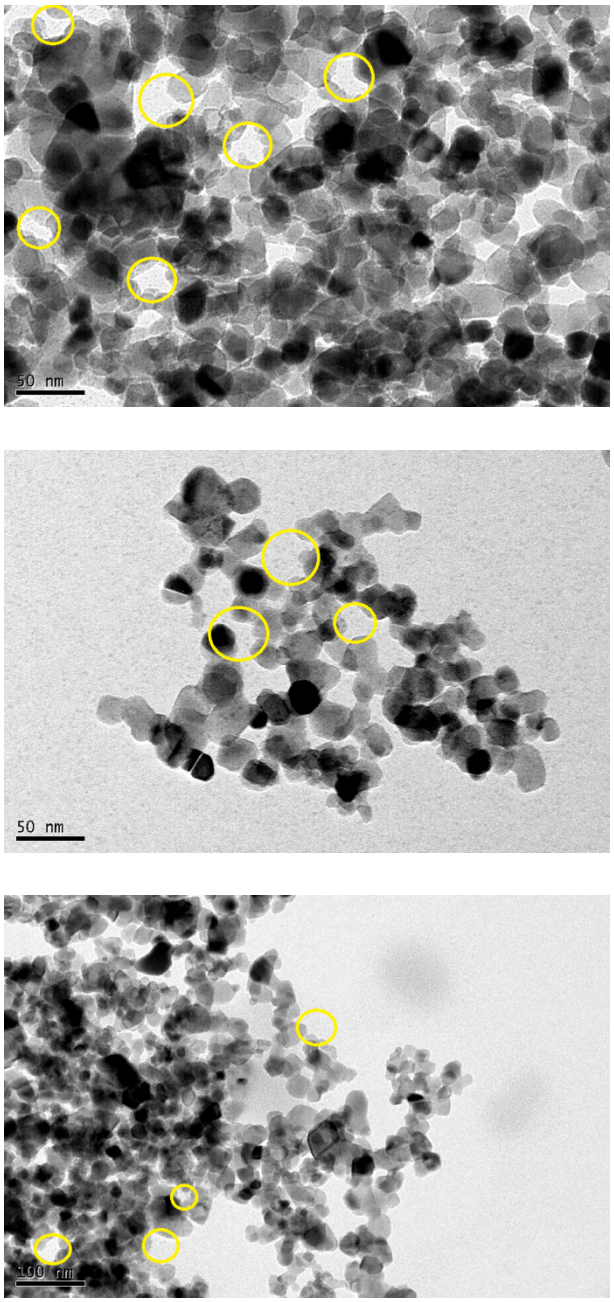

Fig. S2 Some pale contrasts can be observed in the yellow circle areas.

We found that some pale contrasts can be observed in the bright areas as shown in Fig. S2 in yellow circle. In MGT composite, P25 and MoS_2 are actually deposited on graphene sheets, but graphene cannot be fully covered by P25, there must be some "holes" areas that only MoS_2 QDs are deposited, which looks like some pale contrasts appear for the background, but it is actually the P25-free space for MoS_2 QDs. On the other hand, an ultrasonic treatment should be done before TEM measurement, this process

may shake down some of the MoS_2, and it is a little bit like ultrasonic exfoliation process, which may be another reason for the pale contrasts for the background as well.

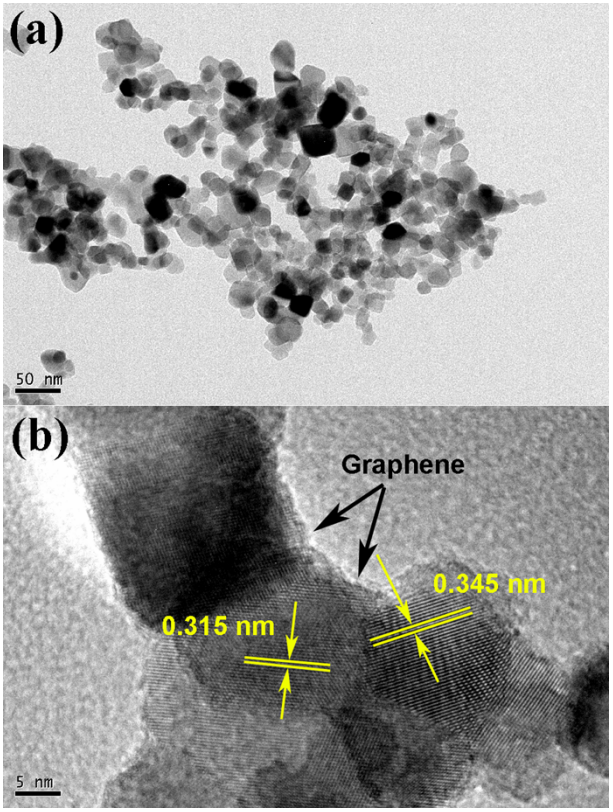

Fig. S3 The TEM (a) and HRTEM (b) image of TiO_2-Graphene without small black dots.

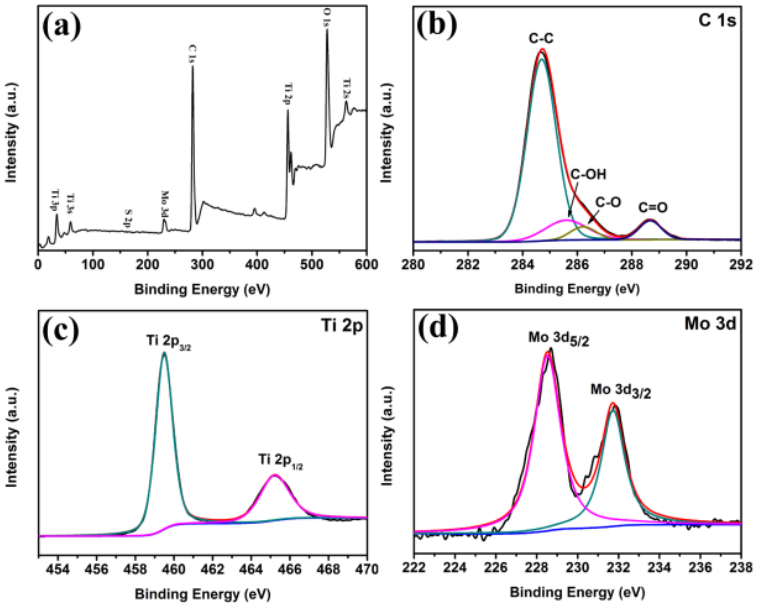

Fig. S4 (a) Full-scale XPS spectrum of MGT-4. Core level XPS spectra of (b) C 1s, (c) Ti 2p and (d) Mo 3d of MGT-4.

Fig. S3a is the full-scale XPS spectrum of MGT-4, which revealed the peaks for Ti, O, Mo, S, and C. The high-resolution XPS spectrum of C 1s in Fig. S2b shows 4 main types of carbon bonds centered at 284.6, 285.7, 286.2 and 288.3 eV are associated with C–C, C–OH, C–O (epoxy/alkoxy), and C=O,[4]respectively, which proves the reduction of GO to graphene compared to the C 1s pattern of GO (see Fig. S4). While the high-resolution XPS spectrum of Ti 2p shows two peaks at 459.0 and 464.9 eV, respectively, which are in good agreement with the reported XPS data of Ti $2p_{3/2}$ and Ti $2p_{1/2}$ in TiO_2. [5] In addition, the binding energies of the Mo $3d_{5/2}$ and Mo $3d_{3/2}$ peaks at 228.9 and 231.9 eV, respectively, which are typical values for Mo^{4+} in MoS_2.[6]

Fig. S5 C1s XPS spectrum of GO.

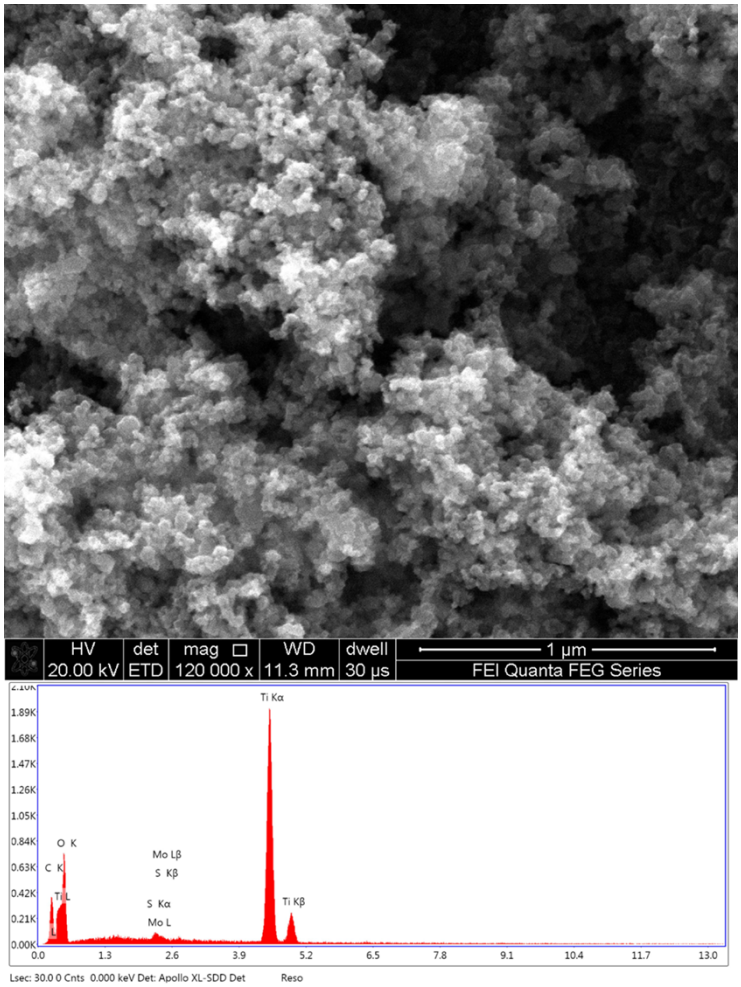

Fig. S6 SEM and the corresponding EDS spectrum of MGT-4

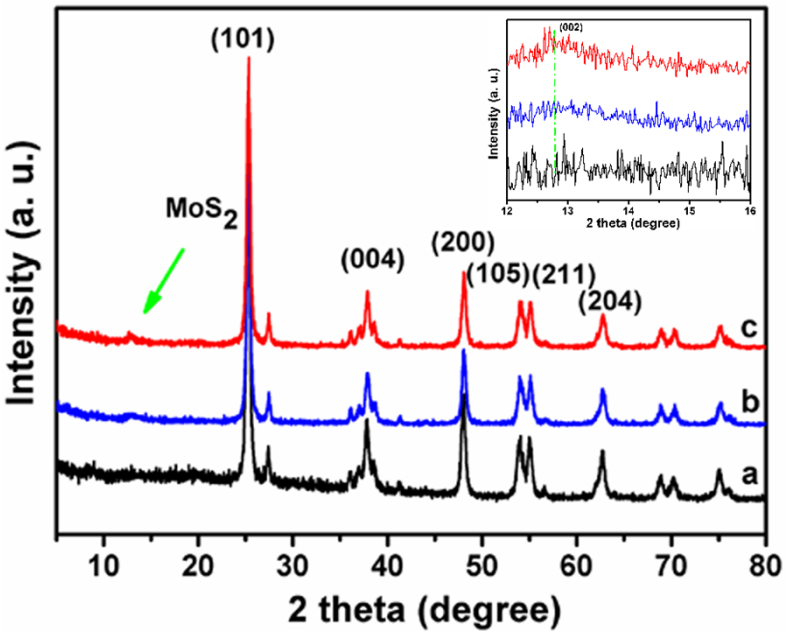

Fig. S7 XRD pattern of (a) TiO_2, (b) TiO_2-Graphene, (c) MGT-4.

Fig. S6 shows the XRD pattern of MGT-4 and take TiO_2 as a reference. The diffraction peaks match those of the crystalline anatase phase of TiO_2, and for MGT-4, the appearance of diffraction peak around 13° is the typical structure of MoS_2,[7] which confirms the presence of MoS_2. The presence of graphene is failed to observe in XRD pattern since it is overlapped by (101) peak of TiO_2,

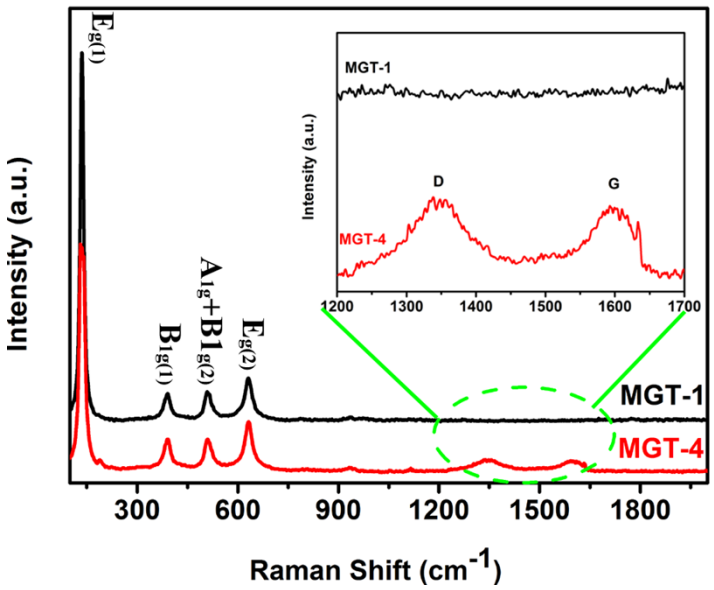

Fig. S8 Raman spectra of MGT-1 and MGT-4.

Fig. S7 shows the Raman spectroscopy measurements of MGT-1 and MGT-4. The Raman spectrum of the MGT-1 and MGT-4 show several characteristic bands at 148, 399, 518, and 639 cm^{-1}, corresponding to the $E_{g(1)}$,$B_{1g(1)}$,A_{1g} +$B_{1g(2)}$, and $E_{g(2)}$ modes of TiO_2, [8] respectively. Clearly, two typical bands at about 1344 cm^{-1} (D band) and 1588 cm^{-1} (G band) for the graphitized structures were also observed, which confirms the presence of graphene in the MGT composite.[9, 10]

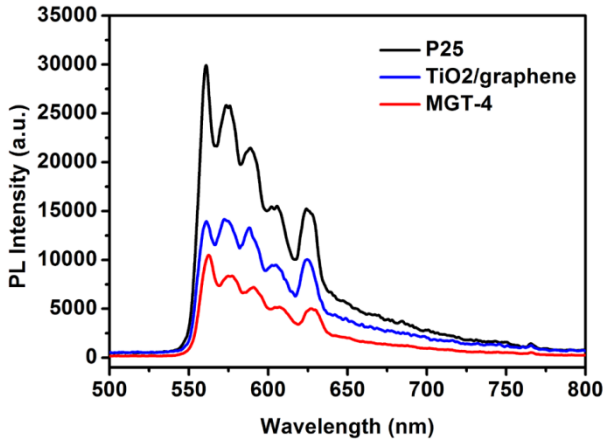

Fig. S9 Photoluminescence spectra of P25, TiO_2/graphene and MGT-4.

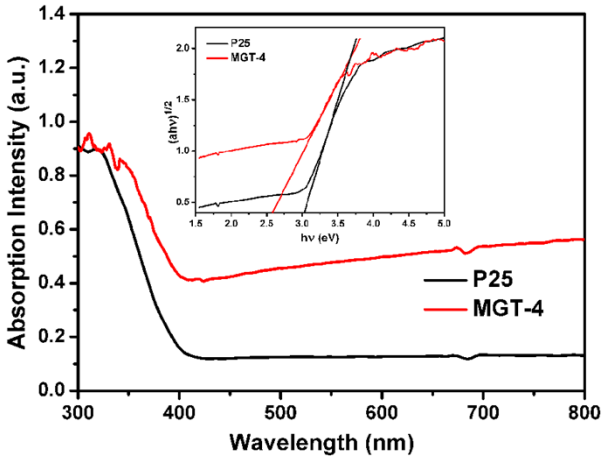

Fig. S10 Diffuse reflectance absorption spectra of P25 and MGT-4, and inset of the plot of transformed kubelka-Munk function *versus* the energy of the light of P25 and MGT-4.

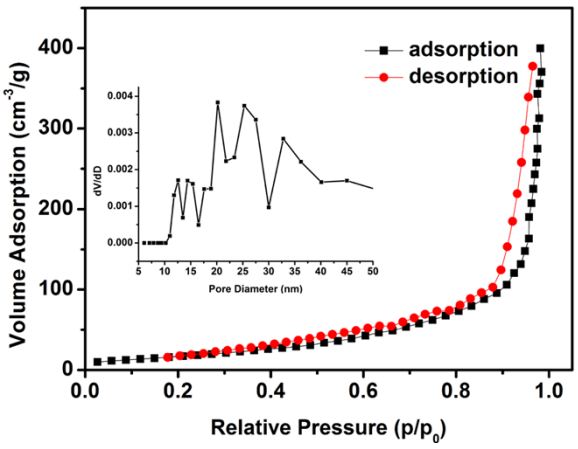

Fig. S11 Typical nitrogen adsorption-desorption isotherm of MGT-4. The insert corresponds to the pore size distribution measured by the BJH method.

Fig. S10 shows a typical nitrogen adsorption–desorption measurements along with the Brunauer–Emmet–Teller (BET) and Barrett–Joyner–Halenda (BJH) methods for MGT-4. According to the IUPAC nomenclature, a type IV isotherm with a H1 hysteresis loop is presented, which was characteristic of the mesoporous material with cylindrical pore geometry present within the MGT-4, and facile connectivity between the pores.[11] Based on the BJH equation from the desorption branch of the isotherm, MGT-4

showed a relatively broad pore size distribution. (inset of Fig. S10) A special surface area of MFT-4 was determined to be 67.8 m^2g^{-1} based on the BET analysis, which was higher than that of the P25 (31.5 m^2g^{-1}).

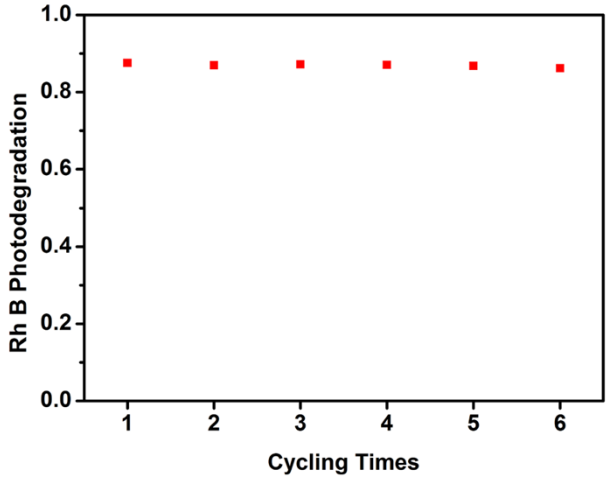

Fig. S12 Cycling degradation rate for Rh B of MGT-4 under simulated sunlight irradiation.

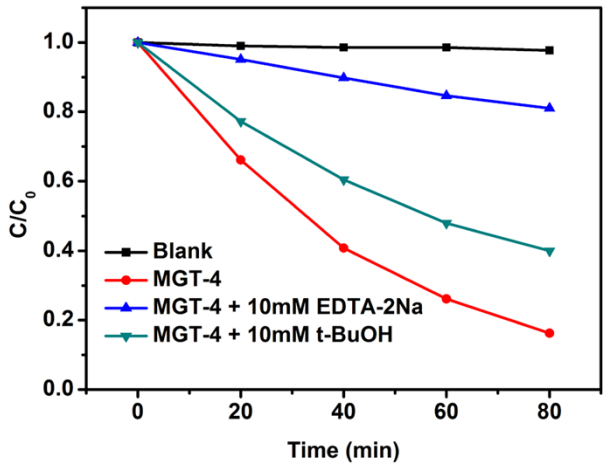

Fig. S13 Trapping test of photogenerated holes and hydroxyl radicals in the MGT-4 composite system.

Table S1. Detailed experimental conditions of MGT samples.

Sample	GO[a] (mg)	Na_2MoO_4•$2H_2O$ (mg)	CN_2H_4S (mg)	P25(g)	DMAc (g)	DI (g)	Time (h)	Temp (°C)
MGT-1	10	0	0	2	20	20	10	150
MGT-2	10	75.5	23.75	2	20	20	10	150
MGT-3	10	105.7	33.25	2	20	20	10	150
MGT-4	10	151	47.5	2	20	20	10	150
MGT-5	10	181.2	57	2	20	20	10	150
MGT-6	10	226.5	71.25	2	20	20	10	150

a: Graphene oxide

Table S2 Parameters obtained from the nitrogen desorption isotherm experiments

Sample	Mean pore size (nm)	Pore volume (cm^3g^{-1})	Surface area (m^2g^{-1})
P25	19.1	0.30	31.5
MGT-1	36.3	0.58	32.2
MGT-4	18.4	0.62	67.8

References:

1. Hummers, W. S.; Offema, R. E. *J. Am. Chem. Soc.,* **1958**, 80, 1339.
2. Park, S. J.; An, J. H.; Jung, I.; Piner, R. D.; An, S. J.; Li, X. S. *Nano Lett.,* **2009**, 9, 1593-1597.
3. Gao,W.; Wang, M.; Ran, C.; Yao, X.; Yang, H.; Liu, J.; He, D.; Bai, J. *Nanoscale,* **2014**,6,5498-5508.
4. Gao, W.; Ran, C.; Wang, M.; Yao, X.; He, D.; Bai, J. *J. Nanopart. Res.*, **2013**, 15, 1727.
5. Zhang, Z.; Xiao, F.; Guo, Y.; Wang, S.; Liu, Y. *ACS Appl. Mater. Interfaces,* **2013**, 5, 2227-2233.
6. Vanchura, B. A.; He, P. G.; Antochshuk, V.; Jaroniec, M.; Ferryman, A.; Barbash, D.; Fulghum, J. E.; Huang, S. D. *J. Am. Chem. Soc.,* **2002**, 124, 12090.
7. Ran, C.; Wang, M.; Gao, W.; Ding, J.; Shi, Y.; Song, X.; Chen, H.; Ren, Z. *J. Phys. Chem. C,* **2012**, 116, 23053.
8. Yu, J.; Ma, T.; Liu, S. *Phys. Chem. Chem. Phys.,* **2011**, 13, 3491-3501.
9. Pimenta, M. A.; Dresselhaus, G.; Dresselhaus, M. S.; Cancado, L. G.; Jorio, A.; Saito, R. *Phys. Chem. Chem. Phys.,* **2007**, 9, 1276-1290.

10. Zhang, W. X.; Cui, J. C.; Tao, C. A.; Wu, Y. G.; Li, Z. P.; Ma, L.; Wen, Y. Q.; Li, G. T. *Angew. Chem. Int. Ed.,* **2009**, 48, 5864-5868.
11. Kruk, M.; Jaroniec, M. *Chem. Mater.,* **2001**, 13, 3169-3183.